1   **Supplementary Material:**

2   **Quasi-static 3D structure of graphene ripple measured using aberration-corrected TEM**

3

4   Yuhiro Segawa,[a,*] Kenji Yamazaki,[a] Jun Yamasaki,[b,c] Kazutoshi Gohara[a,*]

5

6   *[a]Division of Applied Physics, Graduate School of Engineering, Hokkaido University Sapporo*

7   *063-8628, Japan*

8   *[b]Research Center for Ultra-High Voltage Electron Microscopy, Osaka University, 7-1,*

9   *Mihogaoka, Ibaraki, Osaka 567-0047, Japan*

10   *[c]Institute of Materials and Systems for Sustainability, Nagoya University, Furo-cho, Chikusa,*

11   *Nagoya 464-8601, Japan*

12

13   Corresponding Authors:

14   * E-mail: yuhiro26@eis.hokudai.ac.jp (Y.S.)

15   *E-mail: gohara@eng.hokudai.ac.jp (K.G.)

16

10

**Figure S1. The method of determining the defocus value of the six-membered ring of the TEM image.**

This is a graph showing the change in correlation value when the TEM image 6 in Fig. 3a is compared with the six-membered ring of the library. The horizontal axis is the defocus value of the six-membered ring of the library, and the vertical axis is the correlation value. It can be seen that the peak (red plot) is at -30 Å and that the correlation value decreases as the difference from -30 Å increases. In the method used in this paper, the defocus value of the library that becomes the peak is used as the defocus value of the six-membered ring. Only one unique peak appeared and the same was true for all 15 TEM images used for reconstruction. Therefore, the six-membered ring image in the experiment can uniquely determine the defocus value. The accuracy of the determined defocus value is ±1 Å.
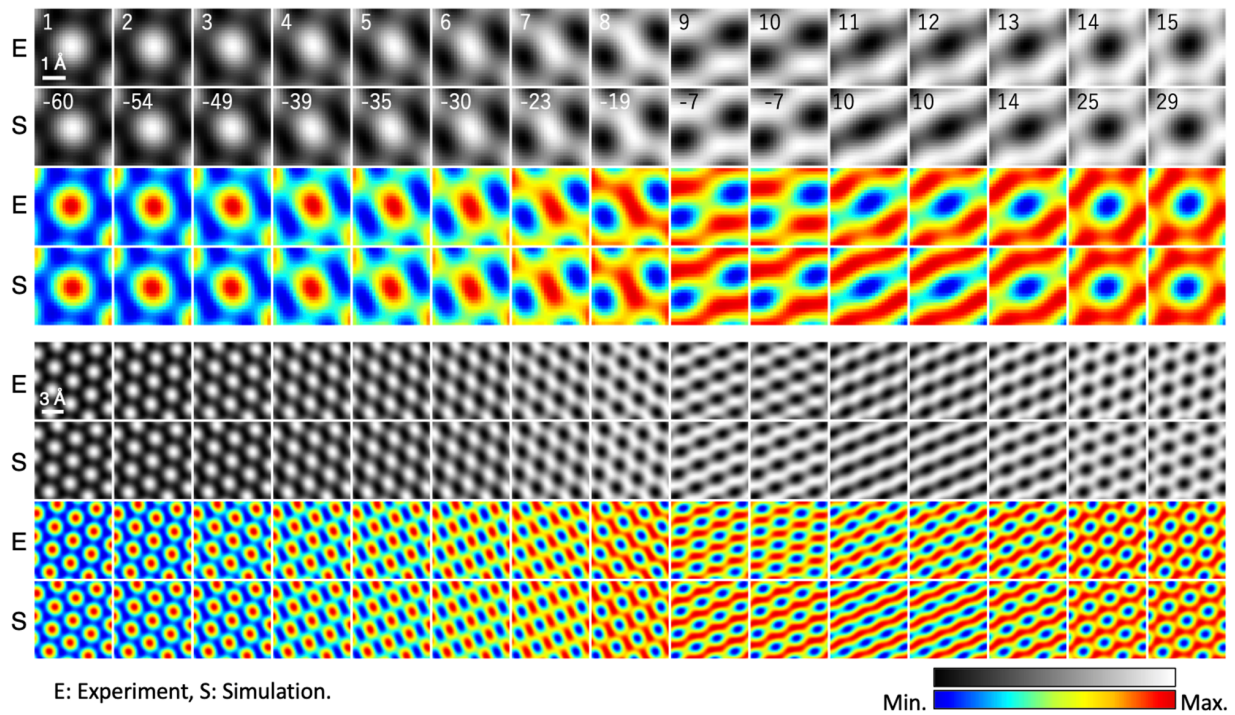
Figure S2. TEM images of six-membered rings.

The sizes of one and seven six-membered rings are presented as the grayscale and pseudo colors, respectively. The grayscale makes it easier to imagine the image obtained by TEM observation. Pseudo colors have the effect of making it easier to see slight contrast differences in the intensities of 2D images.
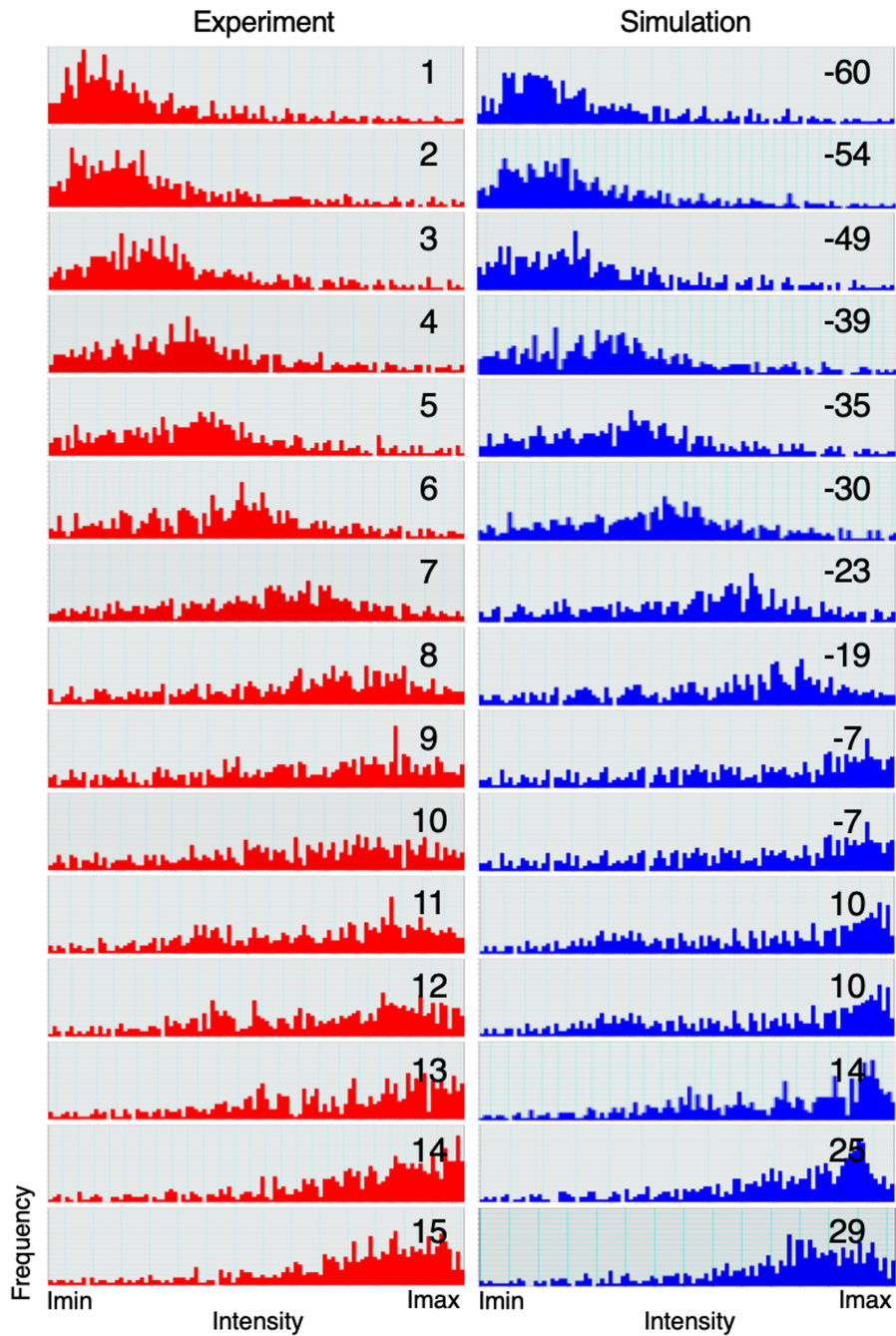
Figure S3. Intensity distribution of TEM images of the six-membered ring.
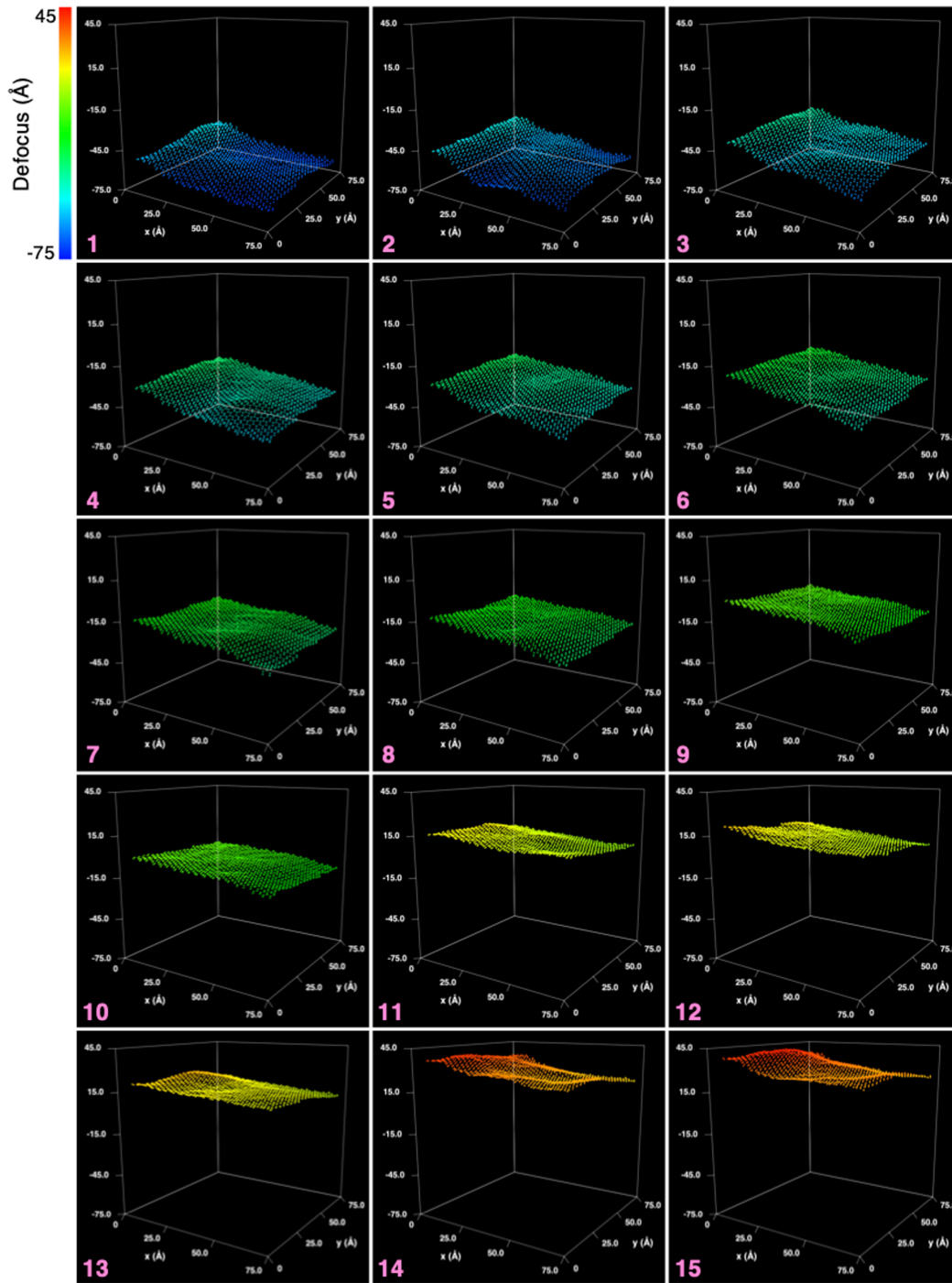
The horizontal and vertical axes represent intensity and frequency, respectively. It was confirmed that the experiment and the simulation were in good agreement also in the intensity distribution of the six-membered ring.
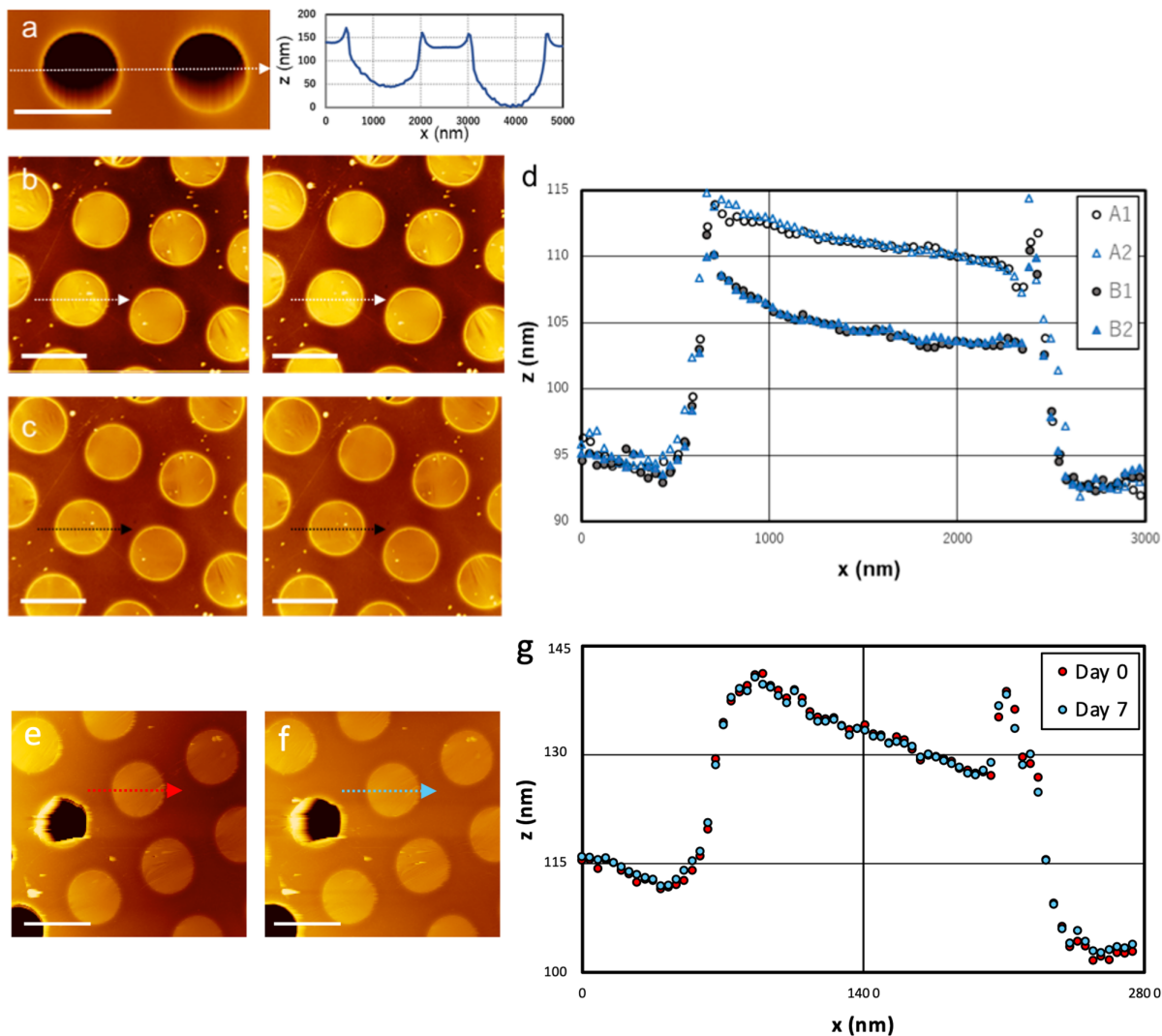
Figure S4. 3D reconstruction of 15 through-focus TEM images.

The vertical axis is defocus (Å).

Figure S5. AFM images and cross-sectional profiles of a TEM grid before and after graphene transfer. All scale bars are 2 μm.

a. An AFM image and a cross-sectional profile of a TEM grid without graphene transfer. Cross-sectional profiles along the straight line indicated by the white arrows in the AFM image. It can be confirmed from the profile that the edge of the hole is raised about 20 nm.

b. Consecutive AFM images of holes with graphene transferred after TEM observation.

c. Consecutive AFM images of holes with graphene transferred before TEM observation. The same area is observed in b.

d. Cross-sectional profiles along the straight line indicated by the white and black arrows in the AFM images of b and c A1 and A2, B1 and B2 are cross-sectional profiles obtained from the first and second observations performed after and before the TEM observation, respectively. The same structure appears in A1 and A2, and B1 and B2 with a difference of 1 nm or less in height.

e. AFM image of holes with graphene transferred. The data are from another specimen that was not observed by TEM.

f. AFM image 7 days after e. The same area is observed in e. The TEM grid was stored in a desiccator during that time.

g. Cross-sectional profiles along the straight line indicated by the red and blue arrows in the AFM images of e and f. The same structure appears in e and f with a difference of 1 nm or less in height. Strictly speaking, the state of the cantilever position and that of the laser irradiation position differ between days 0 and 7. However, since the same structure is measured, subtle differences in measurement conditions do not significantly affect the results.

From the above results, the change (~ 6 nm) shown in this paper is more than the measurement error by AFM and supports the change of the TEM sample.
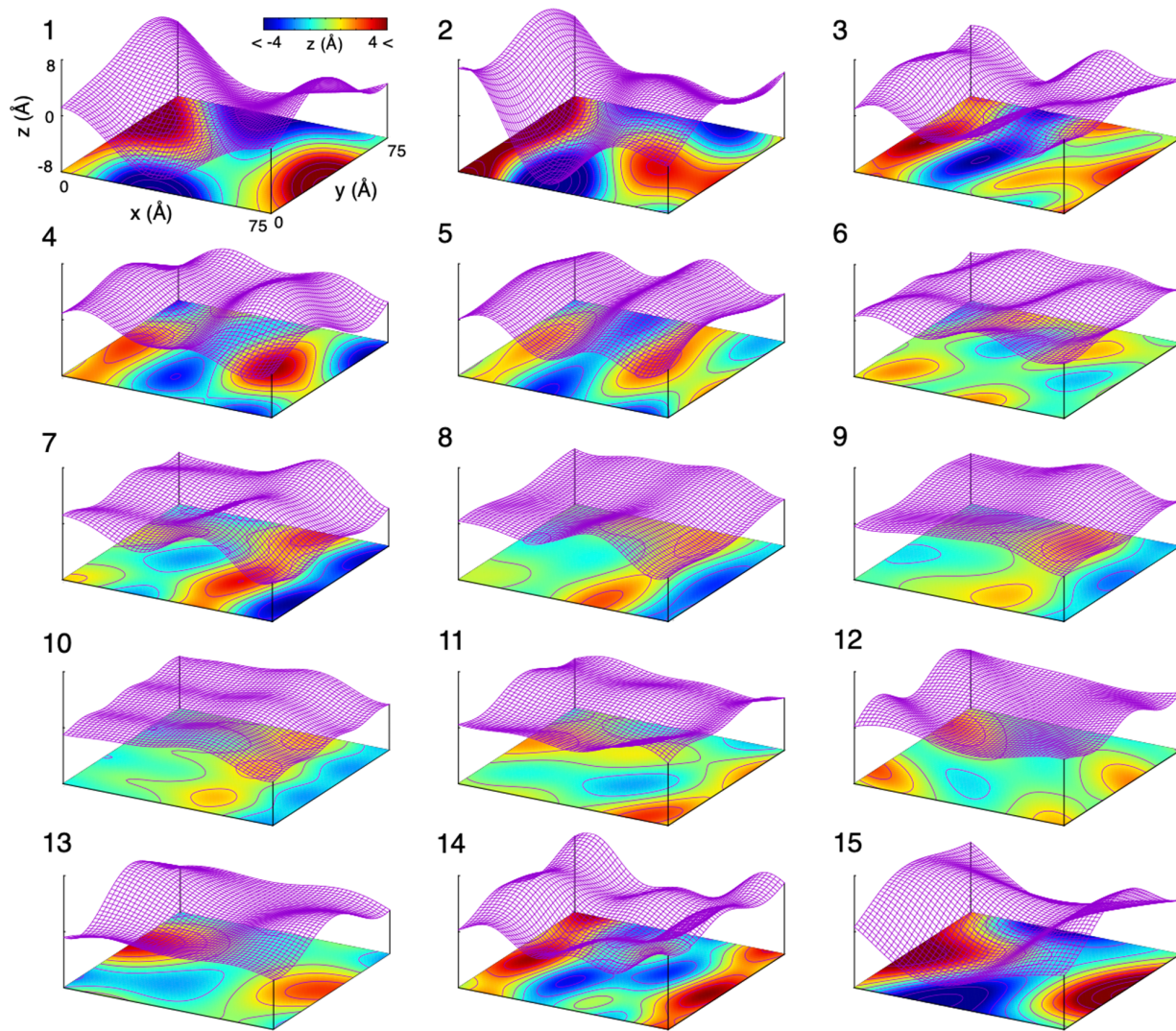
1
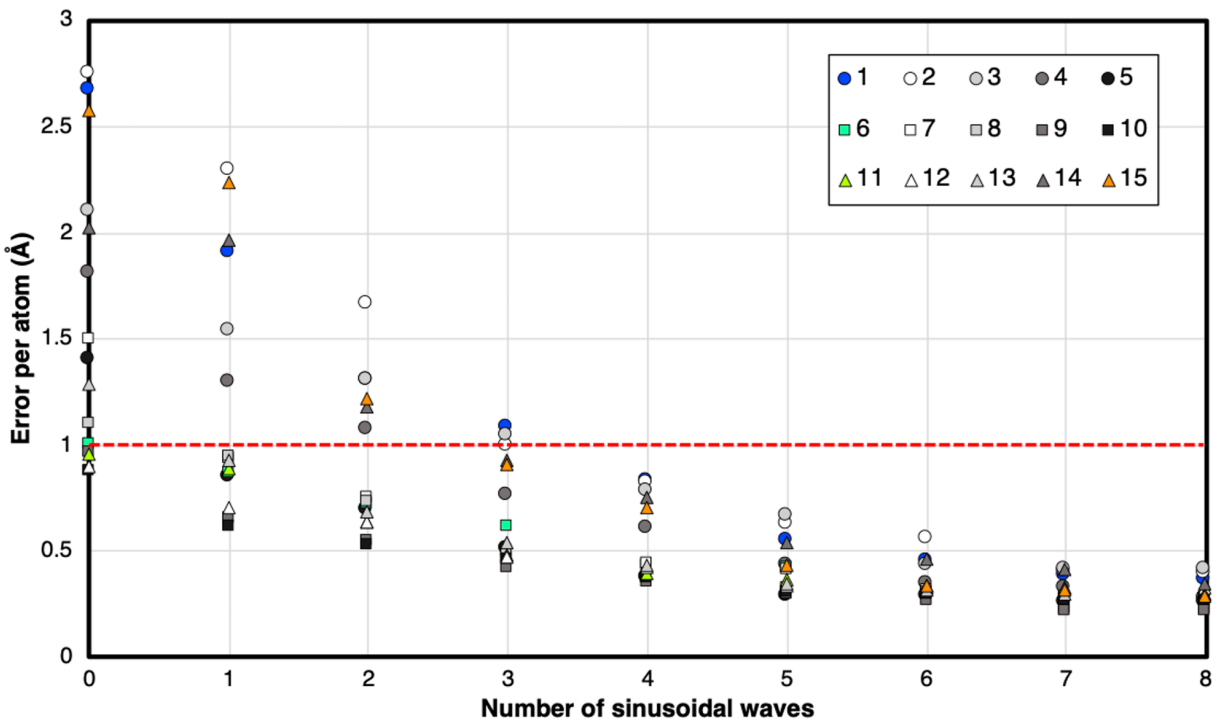
Figure S6. Z error per atom with respect to the number of sinusoidal waves.

The horizontal axis is the number of sinusoidal waves used in the approximation function, and the vertical axis is the z error per atom (Å). The red dotted line shows the standard deviation of the height error 1 Å in the numerical simulation in Fig. 1b.

6

Figure S7. Ripple structures.

Each ripple structure was composed of three sinusoidal waves whose directions corresponded to the vector of the six-membered ring, as shown in Fig. 5g.